THE JOURNAL OF PHYSICAL CHEMISTRY C

Article

pubs.acs.org/JPCC

Quasi-Free Nanoparticle Vibrations in a Highly Compressed ZrO_2 Nanopowder

Lucien Saviot,*[,†] Denis Machon,[‡] Alain Mermet,[§] Daniel B. Murray,[∥] Sergey Adichtchev,[§,⊥] Jérémie Margueritat,[§] Frédéric Demoisson,[†] Moustapha Ariane,[†] and María del Carmen Marco de Lucas[†]

[†]Laboratoire Interdisciplinaire Carnot de Bourgogne, UMR 6303 CNRS-Université de Bourgogne, 9 Av. A. Savary, BP 47 870, F-21078 Dijon Cedex, France

[‡]Université de Lyon, F-69622, France; Université Lyon 1, Laboratoire PMCN, CNRS, UMR 5586, F-69622 Villeurbanne Cedex, France

[§]Université de Lyon, F-69622, France; Université Lyon 1, LPCML, CNRS, UMR 5620, F-69622 Villeurbanne Cedex, France

[∥]Department of Physics, University of British Columbia Okanagan, 3333 University Way, Kelowna, British Columbia, Canada V1 V 1 V7

[⊥]Institute of Automation and Electrometry, Ak. Koptyuga 1, 630090 Novosibirsk, Russia

Supporting Information

ABSTRACT: Several-nanometer-size mechanical oscillators, or nanoresonators, may complement electronic and optical technologies in future terahertz devices, but they can be useful only if they can be made to have relatively light damping, that is, a quality factor as high as possible. Completely mechanically isolated nanoparticles a few nanometers in size would of course be very high-quality factor terahertz nanoresonators but would be totally unsuitable for integration into practical devices. We report the fabrication of solid-embedded nanoparticles whose natural mechanical vibrations have a usefully high quality factor. In this proof-of-concept study, a powder of approximately spherical, monodisperse 5 nm diameter ZrO_2 nanoparticles is compressed to 20 GPa, whereas their mechanical vibrations are directly observed using Raman spectroscopy. Even though they are compressed very tightly in a solid, the individual nanoparticles vibrate essentially independently, being minimally coupled to their neighbors. This mechanical isolation is attributed to a subnanometer-thickness adsorbed water molecule layer, which we theoretically show to be more than sufficient to create a significant impedance mismatch. We also investigated the propagation of sound waves through the nanopowder using Brillouin scattering. The speed of long-wavelength acoustic waves is strongly dependent on the internanoparticle coupling, as revealed by the extreme variation with pressure of the speed of sound. In addition, the low-frequency Raman spectra provide an indication of the solid-state character of nanoscale ZrO_2. There is a transition of the Zr−O bonds from being primarily ionic at low pressures to being primarily covalent at high pressures. Finally, a strong background in these Raman spectra is due to quasielastic scattering, which disappears at high pressure or low temperature.

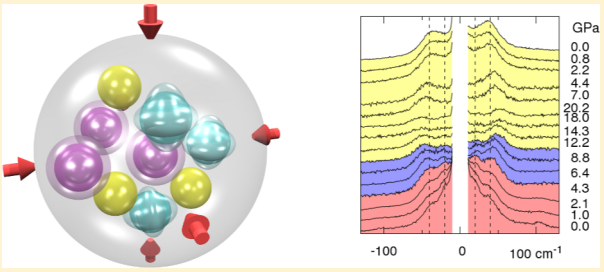

INTRODUCTION

Nanoelectromechanical systems (NEMSs) are a future technological goal in which there is a convergence of mechanical, electrical, and modulated optical signals in single integrated devices operating in the terahertz range.[1] This next generation of devices holds out hope for significant advances over current technology, which is based solely on high integration of transistors communicating via electrical signals. Extremely high density of mechanical devices is possible at such frequencies because an object vibrating at one terahertz is only a few nanometers in size.

The technology of microelectromechanical systems (MEMSs) is already mature but operates at much lower frequencies and involves devices of much larger size. Successive developments of the mechanical oscillators for these devices have attained higher and higher vibrational frequencies, but this has come at the cost of reduction in the quality factor (Q). As Ekinci and Roukes have pointed out, for the best micro-resonators, Q scales as a power law with the volume.[1]

The frequency of the fundamental vibrational mode of a spherical nanoparticle (NP) is roughly the speed of sound divided by the diameter. Thus, NPs a few nanometers across are terahertz nanoresonators. The Raman-active modes[2] can be observed in low-frequency Raman scattering spectra.[3,4] The breathing mode of metallic NPs can be excited, and its damped oscillations can be followed in real time in femtosecond laser pump probe experiments.[5] In all of these cases, Q is relatively low as a result of the rapid loss of vibrational energy due to

Received: July 17, 2012
Revised: September 7, 2012
Published: September 28, 2012

conduction of sound waves away from the NP into the surrounding solid matrix.

It is possible to make a nanoresonator with extremely high Q by suspending a NP in zero gravity, in free fall, suspended in a laser beam inside a liquid,[5] or lightly adhering to a surface.[6] In all of these cases, there is almost no conduction of vibrational energy away from the NP, but for practical NEMS devices, the nanoresonator must be embedded in a solid. In that case, the acoustic impedance of the matrix and the NPs has to be very different to achieve a high Q. However, the requirement to assemble a NEMS device involving such disparate materials provides a challenge to mass-produced monolithic fabrication.

Here we report the fabrication and characterization of a proof-of-concept nanoresonator, which satisfies the primary NEMS device constraints for practical implementation. We found an experimental Q comparable to the extrapolation of the MEMS scaling law of Ekinci and Roukes down to the nanoscale. In addition, we show theoretically how our device could have a significantly higher Q once its parameters are optimized.

Our experimental investigation involves roughly spherical and monodisperse 5 nm ZrO_2 NPs with fundamental vibrational frequency around 1.2 THz. They are embedded in a solid consisting of a highly compressed nanopowder of other ZrO_2 NPs. Extremely high-pressure (up to 20 GPa) measurements in a diamond anvil cell (DAC) are used to study Q as the nanopowder is compressed.

Our measurements were done primarily using low-frequency Raman scattering. There are a number of recent high-pressure Raman studies of similar oxide nanopowders.[7−9] However, these past works have only studied optical phonons whose frequencies are much higher than the fundamental vibrational frequencies, or long-wavelength acoustic phonons, that we have been able to explore. In Raman scattering, the sample is illuminated with a ∼600 THz laser beam. The Raman-scattered light has a frequency shifted up or down by the mechanical vibration frequency, which in our case is on the order of 1.2 THz. We are able to record spectra as close as 0.3 THz from the Rayleigh line before the million-times-weaker Raman scattering is overwhelmed by the line width of the elastic scattering. Our Raman setup is specially designed for this purpose. Such a low-frequency range in Raman studies is nowadays becoming more easily accessible thanks to the availability of narrow notch filters built from volume Bragg gratings.[10,11]

Our remarkable experimental finding is that despite the extreme pressure applied to the nanopowder the NPs continue to vibrate individually approximately as if they were free. For us to come to this surprising conclusion requires two things to be established: First, the observed frequency must closely match the expected vibrational frequency of an isolated NP. Second, the line width of the Raman peak must be narrow so as to indicate that Q is large.

We begin with the first point. The NPs are clusters of atoms, so in reality they are not truly spherical in shape. However, it is well-established that for the purposes of estimating the frequencies it is an accurate idealization to treat the NPs as free, homogeneous, elastically isotropic, continuum spheres.[12,13] The calculation of the vibrational frequencies is an old classical mechanics problem solved by Lamb.[14] The solution takes as its input parameters the radius, density, and elastic constants of the sphere. Over a quarter of a century, many experimental studies have confirmed that these idealizations give, with some interesting exceptions,[15] reasonably accurate frequency estimates. For our nanopowder, the frequency predicted by Lamb is in excellent agreement with the observed frequency over the entire range of pressure.

In our case, good agreement with Lamb's predicted frequency is essential because it confirms that we are always seeing vibrations of the individual NPs as the pressure goes up. We are able to rule out the possibility that the NPs agglomerate into larger objects because these would vibrate at much lower frequencies. Such fusing of NPs would also ruin the monodispersity of size so that there would no longer be a sharp Raman peak.

As for the second point, the Raman peak has a line width. The frequency of the peak is denoted by ω_{peak}. The full width at half-maximum (FWHM) of the peak is denoted by $\Delta\omega$. The sharpness of the peak is quantified by the total quality factor $Q_{total} = \omega_{peak}/\Delta\omega$. There are two separate mechanisms that broaden the Raman peak. The first effect is the distribution of sizes of the NPs in the sample. The second effect is the peak broadening due to the mechanical damping of the vibrations of an NP as its energy of vibration is transmitted to its surroundings. For a monodisperse sample, the quality factor (due to damping alone) is Q_{damp}. For an inhomogeneous sample in which the vibrations are completely undamped, the quality factor is Q_{inh}. Assuming Lorentzian line shapes, these are related through

$$Q_{total}^{-1} = Q_{damp}^{-1} + Q_{inh}^{-1} \quad (1)$$

In the Raman spectrum, Q_{total} is observed. Because the distribution of the NP sizes is known, Q_{inh} can be determined. Put together, Q_{damp} is obtained. The fact that Q_{damp} is high indicates that the vibrations of a single NP are lightly damped.

METHODS

Sample Preparation. Zirconia NPs (ZrO_2) were synthesized under supercritical water conditions from a homemade continuous process as described in a previous work by some of us.[16] The counter-current flow reactor was fed in zirconyl nitrate salt ($ZrO(NO_3)_2$) from Sigma Aldrich (0.05 mol·L^{-1}) and demineralized water using high-pressure pumps. The total flow rate was set up at 60 mol·L^{-1} (water: 20 + 20; salt: 20; residence time: 4 s). The pressure was regulated at 30 MPa and the temperature at 773 K. Then, the suspension was centrifuged and washed with demineralized water under ultrasonication. The sol formed was freeze-dried to reduce the agglomeration of the NPs. Before compaction, the nanopowder had a very low mass density (a few hundred $\mu g/cm^3$) compared with bulk ZrO_2 (5.7 g/cm^3).

Some of the water molecules involved in the synthesis remained adsorbed on the surface of the NPs. They play a key role, as will be explained later.

Transmission electron microscopy (TEM) studies showed a Gaussian distribution of sizes with a peak at 4.9 nm and FWHM 2.9 nm. The TEM images also confirmed that the NPs were nearly spherical. As prepared, the NPs were monoclinic, although at high-pressures their crystal structure changed, as we will discuss later.

Raman and Brillouin Measurements. The Raman setup used for low-frequency measurements is a Renishaw inVia with 532-nm excitation and a BragGrate notch filter from OptiGrate. The Stokes and anti-Stokes Raman spectra were simultaneously recorded down to 10 cm^{-1} with high throughput compared

with multistage devices. The Raman experiments were also repeated on a Horiba T64000 setup. Matching results (not shown here) were obtained for the Stokes side of the spectra. The Brillouin setup is a six-pass tandem Fabry−Perot interferometer with 532-nm excitation. In all measurements, high pressure was produced in a membrane DAC with low-fluorescence diamonds. NPs were placed into a 125 μm chamber drilled in an indented stainless-steel gasket. By intention, no pressure-transmitting medium was used during these experiments so that the powder itself acts as a quasi-hydrostatic pressure-transmitting medium. The fluorescence of ruby was used as a pressure gauge.

RESULTS AND DISCUSSION

The remarkable narrowness of the NP size and shape distributions of our sample is essential to the success of this study. As a result, we can observe very sharp low-frequency Raman peaks. A wider range of sizes (or shapes) of the NPs would badly blur the Raman peak because frequency is inversely proportional to size. Thus, we are starting with a sample that is a prime candidate for a study that uses low-frequency Raman to characterize the changes of the sample, in this case as the pressure is varied. Raman including low-frequency Raman (Figure 1) and Brillouin spectra (see Supporting Information) have been recorded for this powder at pressures P up to ∼20 GPa in a DAC.

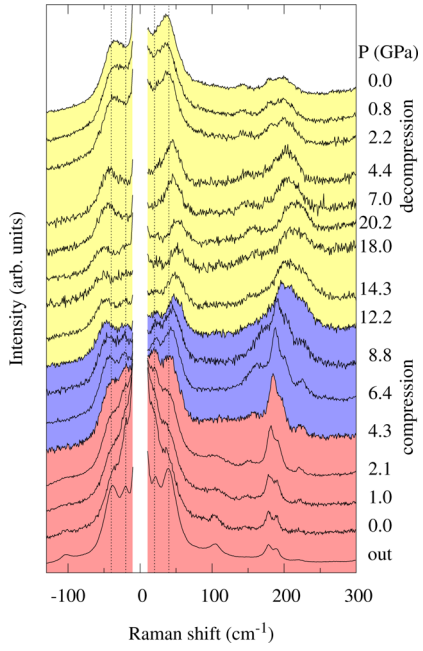

Figure 1. Low-frequency part of the Raman spectra of 5 nm ZrO_2 nanoparticles at high pressure. The spectra were normalized and vertically shifted for clarity. The bottom spectrum (out) is of the as-prepared uncompressed nanopowder prior to insertion into the DAC. Next, from bottom to top, P increases up to ∼20 GPa and then decreases to ambient pressure. The four vertical dashed lines at ±20 and ±40 cm^{-1} are guides to the eye to show the variation of the low-frequency peak positions with P. The crystal lattice structures of ZrO_2 as P increases are indicated with gray shades (colors). The bottom region (medium gray/red) is monoclinic. The next region (dark gray/blue) is orthorhombic I. The next region (light gray/yellow) is orthorhombic II.

Phase Transitions. A detailed analysis of the optical part of the Raman spectra (≳100 cm^{-1}) is outside the scope of this article and will be reported elsewhere, but we provide here a quick overview of the different phase transitions. Bulk ZrO_2 has three crystal structures as P is increased.[17] These transitions are clearly observed in Figure 1. It is initially monoclinic (MI) with a characteristic Raman peak at ∼100 cm^{-1}. At ∼5 GPa it changes to an orthorhombic phase (OI). Finally, at ∼12 GPa it changes to another orthorhombic phase (OII) with a broad Raman peak at ∼200 cm^{-1}. Because the phase transitions observed for our NPs are in good agreement with those of the bulk material and also because the acoustic vibrations of small NPs have been shown to be described accurately with bulk parameters for a variety of systems,[12,13] we will use the elastic parameters for bulk ZrO_2 in the following.[17]

Confined Acoustic Vibrations. *Peak Positions.* We observed at most two low-frequency Raman peaks. Both are due to confined acoustic vibrations in the NPs, which are well-described using the free-sphere model.[14] Under room conditions and for a noncompacted powder these peaks were assigned[16] according to Raman selection rules.[2] The lowest frequency peak is a spheroidal vibration with angular momentum l = 2 denoted S_2^1 in the following. The second peak corresponds to the spheroidal l = 0 mode denoted S_0^1, which involves purely radial (i.e., breathing) motion. The surface motions for these two modes are shown in Figure 2.

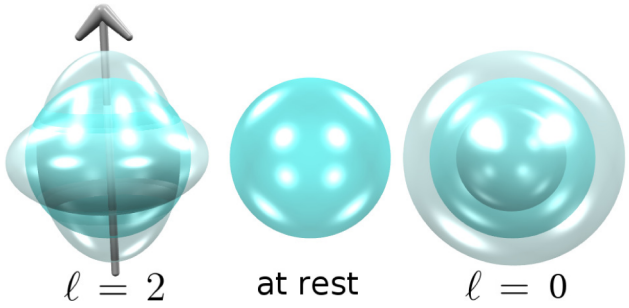

Figure 2. Raman-active Lamb vibrations of a free elastic sphere. The S_2^1 (l = 2) mode is on the left and the breathing S_0^1 (l = 0) mode is on the right. The spheres at the center of the Figure and at the center of the other two representations represent the particle at rest. For both modes, the maximum surface motions are shown. The S_2^1 mode corresponds to stretching, followed by contraction along the z-axis (vertical arrow). The S_0^1 mode is radial expansion and contraction.

The first notable observation regarding the low-frequency Raman peaks is that the two well-resolved peaks in the noncompacted powder (at 21 and 41 cm^{-1} in "out" at the bottom of Figure 1) become blurred in the compacted powder, even at low pressure. The polarized S_0^1 peak is favored in the noncompacted powder because the polarizations of the incident and detected photons are parallel[2] (Figure 3a). Because of multiple scattering, this is no longer the case for the compacted nanopowder, which results in larger relative intensities for the lowest frequency Raman peak (S_2^1) as well as the quasielastic scattering (see later). As will be detailed later, the low-frequency Raman peaks are also not so well-resolved in the compacted powder because the peaks are broadened due to damping of the vibrations. Note that the signal-to-noise ratio in the compacted nanopowder is not as good as in the noncompacted one due to the use of a microscope objective

dx.doi.org/10.1021/jp307066x | J. Phys. Chem. C 2012, 116, 22043−22050

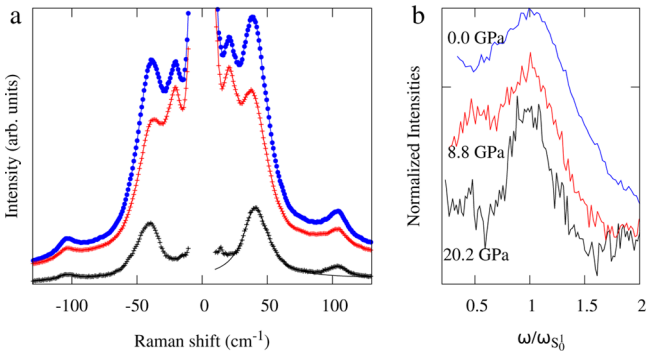

Figure 3. (a) Low-frequency Raman spectra of the uncompressed nanopowder ("out") with the polarizations of the incident and detected photons being parallel (blue dotted curve) and perpendicular (red crossed curve). The weighted difference that cancels the S_2^1 peak reveals the scattering by the S_0^1 peak only (black crosses). The fit of this last curve by a Lorentzian is also shown (black line). (b) Evolution of the S_0^1 peak shape with pressure for the compressed nanopowder. The Raman shifts are normalized to the frequency of the maximum $\omega_{S_0^1}$. The pressures are 20.2, 8.8 (increasing pressure), and 0 GPa (decreasing pressure) from bottom to top. The intensities were normalized after removing a constant background. The spectra are vertically shifted for clarity.

with a large working distance required to study a sample in the DAC.

The positions of the low-frequency Raman peaks change with pressure (Figures 1 and 4a). This is because the density

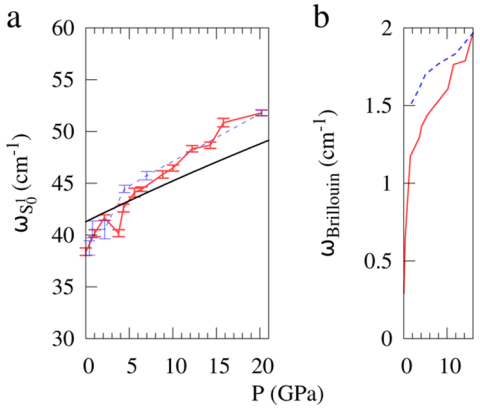

Figure 4. Variation of the S_0^1 (a) and Brillouin (b) peak positions. The frequency variations are plotted with a continuous red curve for increasing P and a dashed blue curve for decreasing P. The breathing vibration S_0^1 frequencies were obtained by fitting the peaks with Lorentzians. The error bars are calculated from the parameter error estimates of the fitting procedure. The black curve corresponds to the calculated variation (see text).

and elastic constants of ZrO_2 change with pressure. The Lamb solution is for a free, homogeneous, elastically isotropic continuum sphere. Approximating our NPs in this way, the frequencies of the S_2^1 and S_0^1 modes are proportional to v_T/R and v_L/R, respectively, the proportionality constants being only very weakly dependent on the sound velocity ratio v_L/v_T.[18] The pressure dependence of the frequencies related to the variation of v_T, v_L, and R with P are as follows: $v_T = (G/\rho)^{1/2}$, $v_L = ((B + (4/3)G)/\rho)^{1/2}$ with $R = ((3M)/(4\pi\rho))^{1/3}$, B and G being the bulk and shear moduli, ρ being the mass density, and M the mass of a spherical NP. The pressure-dependent factors in the positions of the Raman peaks are therefore $G^{1/2}\rho^{-1/6}$ and $(B + (4/3)G)^{1/2}\rho^{-1/6}$ for the S_2^1 and S_0^1 peaks, respectively.

Another potential source of frequency variation could be the change of the shape of the NPs under pressure. Hertz contact mechanics[19] can be used to estimate the deformation of an elastic sphere due to contact with another elastic sphere. As a crude approximation, we assumed that the NPs were perfectly monodisperse and arranged in an fcc structure. Hertz theory predicts that at 20 GPa the NP-NP center-to-center distance is reduced from 5.0 to 4.4 nm. The flat circular facet of contact between two NPs has radius 0.84 nm. Some of us already checked that the frequencies of the S_2^1 and S_0^1 vibrations are only weakly dependent on the exact shape of the NPs as long they are almost spherical, as in cuboctahedra, truncated cuboctahedra, and icosahedra.[20] In particular, for the fcc lattice considered here, the deformed shape has I_h symmetry for which no splitting of the $l = 2$ vibration occurs. Therefore, the model is still valid even for NPs slightly deformed by the applied pressure.

Still another additional potential source of frequency variation when P changes could be related to the medium around each NP. In the following, we will rule out this possibility by showing that the surface of the NPs can be considered to be free whatever P. In a naive picture, we could consider the NPs to be in contact with other NPs everywhere at their surface, leading to a situation without confined vibrations, but the pressure is transmitted to a given NP only through a few point contacts with its closest neighbors. Only part of the surface of the NPs is affected by such contacts leading to the possibility to confine vibrations effectively. In that case, a coupling between the vibrations of neighbor NPs would also increase the measured frequencies.[21,22] However, such a coupling is strongly dependent on the nature of the contact points. In our case, the NPs do not weld together, as confirmed by TEM photos (see Supporting Information).

For our purposes, an essential point is that the NPs are not bare ZrO_2. Molecules of H_2O, N_2, and O_2 adhere to the ZrO_2 surface. Prior to compression, most of the NP surface is surrounded by air, which cannot escape from the leak-proof DAC. The mass of air in the DAC is very small compared with the mass of the nanopowder because air is initially in the gaseous phase with a very low mass density. Therefore, we can safely neglect the N_2 and O_2 molecules in the following. However, the H_2O turns out to play a key role.

In general, nano-oxide surfaces are covered by adsorbed H_2O molecules. The H_2O molecules nearest the ZrO_2 surface are broken apart into an H and an OH group and chemisorbed. Outside this there are physisorbed layers of H_2O. Considering both chemisorption and physisorption, monoclinic zirconia NPs are covered by about three monolayers of H_2O under ambient conditions.[23] For conciseness, in the remainder of this article the word "water" will refer to these few monolayers of H_2O that coat the ZrO_2 surface. Crucially, note that the word "water" does not refer to "bulk liquid water". In addition, the physical properties of this "water" is quite different from that of macroscopic samples of bulk thermodynamic phases of H_2O.

The water can have a dramatic influence on the vibrations of small NPs, as highlighted in Figure 5a. There, we plot the S_0^1 and S_2^1 quality factors (Q_{damp}) of a 5 nm ZrO_2 NP surrounded by a water shell of thickness d and embedded in a ZrO_2 matrix following the method presented in ref 24. This model overestimates the effect of the surrounding NPs by assuming a complete embedding in a ZrO_2 matrix. We used room

dx.doi.org/10.1021/jp307066x | J. Phys. Chem. C 2012, 116, 22043−22050

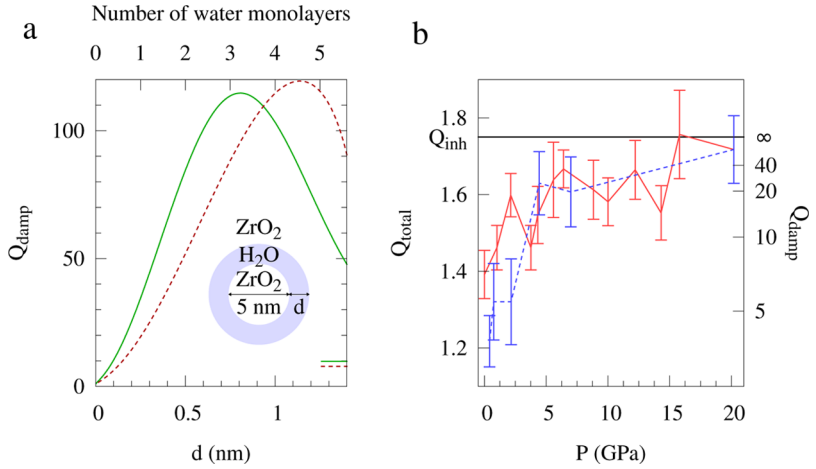

Figure 5. (a) Calculated influence of a water shell (thickness d) on the quality factor Q_{damp} of the vibrations of a 5-nm ZrO_2 NP embedded in ZrO_2. The S_0^1 and S_2^1 vibrations are plotted with a green continuous line and a red dashed line, respectively. The horizontal lines at the lower right corner of the Figure correspond to the case of the same NP in an infinite block of ice. (b) Total quality factor of the S_0^1 Raman peak as a function of pressure with the same color and style as in Figure 4a. Smaller differences between Q_{total} and Q_{inh} correspond to higher Q_{damp}.

condition parameters for monoclinic ZrO_2 for the calculation. For the water, in the absence of other information we used the physical parameters for bulk ice because bulk liquid water turns into bulk ice at pressures that are attained quite early in our high-pressure experiment and also because the water coating the NP will have very different properties from bulk liquid water. When $d = 0$, that is, without the water shell, there are no confined acoustic vibrations (quality factor $Q_{damp} = 0$). With a very thick water shell, the vibrations would be damped with $Q_{damp} \simeq 10$, as for a matrix with the density and elastic properties of bulk ice (horizontal lines at the lower right corner of Figure 5a), but with a water shell a few monolayers thick, the vibrations are lightly damped and theoretically could have a much larger quality factor (up to $Q_{damp} > 100$ for both S_0^1 and S_2^1). One water monolayer is enough to have a dramatic influence on the system due to the small size of the NPs. This is partially because the acoustic impedance mismatch between ZrO_2 and the water is large and also because of constructive interference between the acoustic waves reflected by both interfaces of the water shell.[25] The actual Q_{damp} may be larger in our experiment because the effect of the surrounding NPs has been overestimated in our model by considering an embedding ZrO_2 matrix. The frequencies of the two vibrations do not change significantly with the water shell thickness and remain close to the frequencies of a free sphere. This explains why quasi-free vibrations are possible in this system even at high-pressure. It also explains why the low-frequency Raman peaks remain narrow as they are primarily broadened by the sample size distribution.

For simplicity, our theoretical discussion has been in terms of a nanopowder consisting of NPs all of the same size. The actual sample has a range of sizes. We have carried out simplified molecular dynamics simulations of the process by which the loosely packed nanopowder is compressed. Because each NP is coated with several layers of adsorbed water, it is reasonable to approximate their contact as frictionless. During the very stages of the compression, the NPs rearrange themselves so as to make the density nearly uniform, leaving only very small voids. When the nanopowder is additionally compressed, each NP feels approximately the same pressure. In particular, large NPs and small NPs are approximately equally compressed. Therefore, the size distribution of the highly compressed nanopowder is approximately the same as that of the uncompressed nanopowder, except that the size is rescaled.

Our experiments very clearly show that the breathing mode Raman peak position shifts to higher frequencies as P increases. Figure 4a was obtained by fitting the experimental spectra with one Lorentzian for each peak, the frequencies and widths of the anti-Stokes peaks being fixed as those of the Stokes peaks. One additional Lorentzian centered at zero frequency was used to take into account the quasielastic contribution (see later). A log-normal line shape was used in ref 16. In the present work, the quasi-elastic peak is seen to play a significant role, and by taking it into account an asymmetric line shape is no longer required. This shift reverses when P is brought back down. This indicates that the effect of compressing the nanopowder is governed by the variation of the elastic parameters with P and not by a change in the mass of the NPs, as confirmed by TEM photos (see Supporting Information). Assuming the mass of the NPs to be constant and using the bulk and shear moduli for the OII phase[17] (which is observed during the last half of the compression and during all the decompression) and the third-order Birch–Murnaghan equations of state,[26] we were able to calculate the breathing vibration frequency at all pressures (Figure 4a). The resulting theoretical curve is in good agreement with the experimental 25% variation of the breathing mode frequency.

For comparison, the position of the longitudinal Brillouin peak as a function of P is also plotted in Figure 4b. Clearly the Brillouin signal of the nanopowder, although of acoustic nature, does not conform to that of the NP confined acoustic modes. In these measurements, the Brillouin frequency $\omega_{Brillouin}$ is proportional to the longitudinal speed of sound in the nanopowder. Figure 4b shows a strong increase in $\omega_{Brillouin}$ as P is increased. However, $\omega_{Brillouin}$ does not decrease by so much when P goes back down.[27] In other words, the application of high pressure has an irreversible effect on the nanopowder. Physically, this can be understood. Whether the adhesions between NPs are very loose or very tight makes a big difference to the bulk speed of sound. The initial nanopowder is loosely agglomerated and has a low density. Application of high P would force the NPs tightly together. It is no surprise that the NPs do not become unagglomerated after P goes back down because they would be strongly glued together by the thin

dx.doi.org/10.1021/jp307066x | J. Phys. Chem. C 2012, 116, 22043–22050

water layer. By contrast, the application of high pressure has no irreversible effect on the vibrations of individual NPs. This is due to the acoustic coupling between NPs, which is weak at both low and high P.

Peak Shapes and Q_{damp} Factor. The line width of the Raman peaks also changes rapidly as the nanopowder is compacted. This can be clearly seen in Figure 3b where the Raman shifts are rescaled. The peak shape should be constant for a Raman peak inhomogeneously broadened by the NPs distribution only. However the experimental spectra show a decrease in the line width with increasing pressure for the compressed nanopowder. This points toward a decrease in the homogeneous width, that is, an increase of the quality factor of the vibrations. The same fit of the spectra as before enables us to quantify the quality factor $Q_{total} = \omega_{peak}/\Delta\omega$ of the ensemble of NPs from this broadening (Figure 5b), where ω_{peak} is the Raman peak frequency and $\Delta\omega$ is its FWHM. The inhomogeneous contribution to Q_{total} due to the size and shape distribution of the NPs (Q_{inh}) can be determined from the noncompacted spectrum by assuming that the vibrations are not damped in this case. We obtained $Q_{inh} \simeq 1.75$ by fitting the weighted difference of the parallel and crossed spectra of the uncompressed nanopowder (see Figure 3a). This difference cancels out the S_2^1 Raman peak so that the fit of the line shape of the S_0^1 peak is more reliable. As a completely independent check, the same value was also obtained using the size distribution determined by TEM and the model for the low-frequency Raman intensity presented in ref 16. Then, the quality factor Q_{damp} of the vibration of a single NP can be determined from the relation $Q_{total}^{-1} = Q_{inh}^{-1} + Q_{damp}^{-1}$.

At low pressure, $Q_{total} < Q_{inh}$, resulting in $Q_{damp} \simeq 5$. As P is increased, Q_{total} decreases and becomes much closer to Q_{inh}. This means that Q_{damp} is significantly larger at high pressure. The actual value of Q_{damp} is very uncertain because it is the reciprocal of the difference of two approximately equal numbers. However, a rough estimate indicates that $Q_{damp} \approx 30$ at high pressure. The variation of Q_{damp} (and the better mechanical isolation at the S_0^1 mode frequency) may be attributed to the changes of the water layer. Increased pressure could, in principle, change the thickness, density, and elastic properties of the water layer. To our knowledge, there is no available information to quantify these changes. Even so, whatever these changes are, they will certainly modify the acoustic isolation between NPs. According to our experimental data, the isolation (at the S_0^1 frequency) is improved.

Taking the scaling law of Ekinci and Roukes[1] for Q_{damp} versus resonator volume and extrapolating to a sphere of radius 2.5 nm, Q_{damp} would be ~60. Thus, the Q_{damp} of 30 that we found is roughly what would be expected.

Ionicity/Covalency of the Zr−O Bonds. The S_2^1 peak frequency is also expected to increase with P due to the variation of the parameters. The calculated frequency shift is ~2 cm^{-1} when increasing P from 0 to 12 GPa where it is observed. This shift could not be confirmed experimentally because it is small, partially masked by the intense quasielastic peak below 5 GPa (see later), and also strongly affected by elastic anisotropy.[15,16,20] For the same reasons, the value of Q_{damp} could not be estimated for this vibration.

However, the mere presence of this Raman peak is of interest. As can be seen in Figure 1, the S_2^1 peak is clearly seen as P goes up from 4 to 12 GPa, whereas it appears as a poorly resolved shoulder at lower pressures, but S_2^1 is not observed at 20 GPa as well as when P decreases. Figure 6a shows two spectra obtained at about $P \simeq 7$ GPa when increasing and decreasing the pressure. When P is increased the crystal is OI, but when P is decreased the crystal is OII. We expect that the Zr−O bonds become more covalent as atoms get closer and electronic orbitals overlap more.[28] Mattarelli et al.[29] suggested that the S_2^1 to S_0^1 peak intensity ratio decreases as the bond becomes more covalent by calculating the Raman peak intensities using a dipole−induced dipole mechanism representative of ionic crystal systems and a bond polarizability mechanism for covalent crystal systems. Our experimental results provide a clear support of this trend because only the nature of the Zr−O bonds is changed in our case and not the size or shape distributions of the NPs nor their environment.

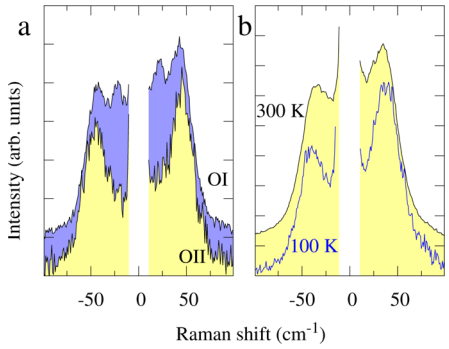

Figure 6. Crystal ionicity and temperature dependence of the low-frequency spectra. (a) Spectra at 6.4 GPa while increasing the pressure (top) and at 7.0 GPa while decreasing the pressure (bottom). (b) Spectra at 300 (top) and 100 K (bottom) of the sample after the high-pressure treatment. The spectra were normalized and vertically shifted for clarity.

Quasielastic Scattering. Quasielastic scattering is a process by which photons are inelastically scattered from the sample, but it differs in mechanism from the Raman scattering that interests us. It occurs at frequencies in between the Rayleigh peak and the region where our Raman peaks start to occur.

An intense quasielastic signal is observed in Figure 1. Its intensity vanishes above ~5 GPa and it reappears at about the same pressure when the pressure decreases. We attribute it to fast relaxation motions, as is commonly observed in non-compact systems such as glasses and liquids.[30] It involves surface atoms including adsorbed species such as H_2O. The quasielastic signal is known to become less intense when P is increased,[31] as we found. It is also known to become less intense when temperature decreases. To check that point, we did low-temperature $T = 100$ K measurements after P was decreased back to room pressure (Figure 6b). The gap between the S_0^1 peak and the elastic peak is better resolved at low temperature. This supports the assignment as a quasielastic signal whose intensity decreases with both decreasing temperature and increasing pressure.

CONCLUSIONS

There has been no previous study of confined acoustic phonons in a compressed nanopowder. This was only possible here due to three things simultaneously working to our advantage. First, we were able to work with a nanopowder sample, which gives strong and sharp low-frequency Raman features. Second, the NPs are small enough so that those peaks are in the terahertz frequency range. Third, we were able to study the nanopowder

dx.doi.org/10.1021/jp307066x | J. Phys. Chem. C 2012, 116, 22043−22050

at extremely high pressures without making use of a pressure-transmitting medium.

In terms of our findings, the big surprise was that the individual NPs vibrate nearly freely, or, in other words, that they have a remarkably high Q_{damp} given their small size and the fact that they are embedded in a solid. Using the same Raman measurements, but looking at the higher frequency range above 100 cm^{-1}, we are very easily able to follow the two crystal structure phrase transitions that occur as the pressure is increased, which confirms that they are essentially the same as in bulk ZrO_2.

It should be emphasized that the attribution of our experimental results to nearly free vibration of individual NPs has been confirmed in two independent ways. First, the vibration frequency, as observed by low-frequency Raman scattering, matches that predicted from the size, density, and elastic constants of the NPs, corrected for the increased pressure. Second, the narrow peaks in the Raman spectrum (whose position matches the NP vibration frequency) can be attributed only to vibrations with a high quality factor.

An unexpected finding is that we were able to see a transition in the nature of the Zr−O bonds from primarily ionic to primarily covalent, which will provide a challenge for theoretical studies.

Crucially, however, our theoretical analysis predicts that the thickness of the layer of H_2O separating NPs has a strong effect on Q_{damp}, with the weakest damping when there is constructive interference in the back-reflected waves. Thus, it is of great importance to carry out future studies in which the amount of adsorbed H_2O on the NPs is varied. We expect that this can be accomplished by varying the temperature and humidity during the nanopowder compression.

The phenomenological power law variation of Q_{damp} with oscillator volume for microscale devices reported by Ekinci and Roukes and extrapolated to our NPs gives $Q_{damp} \approx 60$. What we obtained experimentally was $Q_{damp} \approx 30$. We theoretically showed that Q_{damp} could exceed 100 if the thickness of the H_2O layer separating NPs could be optimized so as to minimize energy transmission. The fact that we have simultaneously seen high Q_{damp} and high frequency in such an easily synthesized sample is noteworthy.

The success of this proof-of-concept study opens the door to applications of such terahertz nanoresonators in NEMS devices. These structures, including the surrounding supporting matrix, are only nanometers in size. It is not necessary to achieve an acoustic impedance mismatch by using more than one material, which is a significant advantage in practical device fabrication. Apart from ZrO_2, many materials would be potential candidates for this acoustic confinement effect because molecular adsorption on surfaces is ubiquitous, whether in molecular form or as chemisorbed radicals. Taken together, these factors give designers of future nanophononic devices wide latitude in selection of materials and fabrication processes.

■ ASSOCIATED CONTENT

Supporting Information

TEM photos before and after the high-pressure treatment and Brillouin spectra as a function of pressure. This material is available free of charge via the Internet at http://pubs.acs.org/.

■ AUTHOR INFORMATION

Corresponding Author

*E-mail: lucien.saviot@u-bourgogne.fr.

Notes

The authors declare no competing financial interest.

■ ACKNOWLEDGMENTS

L.S., M.A., F.D. and M.C.M.L. acknowledge support from Conseil Régional de Bourgogne.

■ REFERENCES

(1) Ekinci, K. L.; Roukes, M. L. *Rev. Sci. Instrum.* **2005**, *76*, 061101-1−061101-12.
(2) Duval, E. *Phys. Rev. B* **1992**, *46*, 5795−5797.
(3) Duval, E.; Boukenter, A.; Champagnon, B. *Phys. Rev. Lett.* **1986**, *56*, 2052−2055.
(4) Saviot, L.; Mermet, A.; Duval, E. In *Nanoparticles and Quantum Dots*; Sattler, K. D., Ed.; Handbook of Nanophysics; CRC Press: Boca Raton, FL, 2010; Chapter 11.
(5) Ruijgrok, P. V.; Zijlstra, P.; Tchebotareva, A. L.; Orrit, M. *Nano Lett.* **2012**, *12*, 1063−1069.
(6) Tchebotareva, A. L.; van Dijk, M. A.; Ruijgrok, P. V.; Fokkema, V.; Hesselberth, M. H. S.; Lippitz, M.; Orrit, M. *ChemPhysChem* **2009**, *10*, 111−114.
(7) Liu, B.; Yao, M.; Liu, B.; Li, Z.; Liu, R.; Li, Q.; Li, D.; Zou, B.; Cui, T.; Zou, G.; Liu, J.; Chen, Z. *J. Phys. Chem. C* **2011**, *115*, 4546−4551.
(8) Dogra, S.; Sharma, N. D.; Singh, J.; Poswal, H. K.; Sharma, S. M.; Bandyopadhyay, A. K. *High Pressure Res.* **2011**, *31*, 292−303.
(9) Machon, D.; Daniel, M.; Bouvier, P.; Daniele, S.; Le Floch, S.; Melinon, P.; Pischedda, V. *J. Phys. Chem. C* **2011**, *115*, 22286−22291.
(10) Lebedkin, S.; Blum, C.; Sturzl, N.; Hennrich, F.; Kappes, M. M. *Rev. Sci. Instrum.* **2011**, *82*, 013705-1−013705-6.
(11) Tan, P. H.; Han, W. P.; Zhao, W. J.; Wu, Z. H.; Chang, K.; Wang, H.; Wang, Y. F.; Bonini, N.; Marzari, N.; Pugno, N.; Savini, G.; Lombardo, A.; Ferrari, A. C. *Nat. Mater.* **2012**, *11*, 294−300.
(12) Combe, N.; Huntzinger, J. R.; Mlayah, A. *Phys. Rev. B* **2007**, *76*, 205425-1−205425-12.
(13) Combe, N.; Chassaing, P.-M.; Demangeot, F. *Phys. Rev. B* **2009**, *79*, 045408-1−045408-9.
(14) Lamb, H. *Proc. London Math. Soc.* **1881**, *s1−13*, 189−212.
(15) Portalès, H.; Goubet, N.; Saviot, L.; Adichtchev, S.; Murray, D. B.; Mermet, A.; Duval, E.; Piléni, M.-P. *Proc. Natl. Acad. Sci. U.S.A* **2008**, *105*, 14784−14789.
(16) Demoisson, F.; Ariane, M.; Saviot, L. *J. Phys. Chem. C* **2011**, *115*, 14571−14575.
(17) Ren, H.; Zhu, B.; Zhu, J.; Hao, Y.; Yu, B.; Li, Y. *Solid State Sci.* **2011**, *13*, 938−943.
(18) Saviot, L.; Murray, D. B. *Phys. Rev. B* **2005**, *72*, 205433-1−205433-6.
(19) Johnson, K. L. *Contact Mechanics*; Cambridge University Press: London, 1987.
(20) Saviot, L.; Murray, D. B. *Phys. Rev. B* **2009**, *79*, 214101-1−214101-11.
(21) Saviot, L.; Murray, D. B. *Phys. Rev. B* **2010**, *81*, 235432-1−235432-7.
(22) Mattarelli, M.; Montagna, M.; Still, T.; Schneider, D.; Fytas, G. *Soft Matter* **2012**, *8*, 4235−4243.
(23) Radha, A. V.; Bomati-Miguel, O.; Ushakov, S. V.; Navrotsky, A.; Tartaj, P. *J. Am. Ceram. Soc.* **2009**, *92*, 133−140.
(24) Saviot, L.; Murray, D. B. *Phys. Rev. Lett.* **2004**, *93*, 055506-1−055506-4.
(25) Mongin, D.; Juvé, V.; Maioli, P.; Crut, A.; Del Fatti, N.; Vallée, F.; Sánchez-Iglesias, A.; Pastoriza-Santos, I.; Liz-Marzán, L. M. *Nano Lett.* **2011**, *11*, 3016−3021.
(26) Birch, F. *Phys. Rev.* **1947**, *71*, 809−824.
(27) Marquardt, H.; Gleason, A.; Marquardt, K.; Speziale, S.; Miyagi, L.; Neusser, G.; Wenk, H.-R.; Jeanloz, R. *Phys. Rev. B* **2011**, *84*, 064131-1−064131-9.
(28) Liu, C.-Y.; Bard, A. J. *Nature* **2002**, *418*, 162−164.

(29) Mattarelli, M.; Montagna, M.; Rossi, F.; Chiasera, A.; Ferrari, M. *Phys. Rev. B* **2006**, *74*, 153412-1−153412-4.
(30) Novikov, V. N.; Sokolov, A. P.; Strube, B.; Surovtsev, N. V.; Duval, E.; Mermet, A. *J. Chem. Phys.* **1997**, *107*, 1057−1065.
(31) Hong, L.; Begen, B.; Kisliuk, A.; Pawlus, S.; Paluch, M.; Sokolov, A. P. *Phys. Rev. Lett.* **2009**, *102*, 145502-1−145502-4.